Surface stress-induced change in overall elastic behavior and self-bending of ultrathin cantilever plates

H. Sadeghian,[1,2,a)] J. F. L. Goosen,[1] A. Bossche,[2] and F. van Keulen[1]
[1]*Structural Optimization and Computational Mechanics (SOCM) Group, Department of Precision and Microsystems Engineering, Delft University of Technology, Mekelweg 2, Delft, Zuid Holland 2628 CD, The Netherlands*
[2]*Electronic Instrumentation Laboratory, Delft University of Technology, Mekelweg 4, Delft, Zuid Holland 2628 CD, The Netherlands*

(Received 10 April 2009; accepted 21 May 2009; published online 9 June 2009)

In this letter, the dominant role of surface stress and surface elasticity on the overall elastic behavior of ultrathin cantilever plates is studied. A general framework based on two-dimensional plane-stress analysis is presented. Because of either surface reconstruction or molecular adsorption, there exists a surface stress and a surface elasticity imbalance between top and bottom surface of the cantilever. The surface elasticity imbalance creates an extra bending-extensional coupling which has not been taken into account previously. This leads to a modified extensional stiffness, bending stiffness and bending-extensional coupling stiffness. Due to the surface stress imbalance, an extended Stoney's formula for self-bending of ultrathin cantilevers is derived. © *2009 American Institute of Physics*. [DOI: 10.1063/1.3153158]

The mechanical behavior of nanostructures and specifically ultrathin cantilevers, is of considerable interest due to their potential applications. Previous studies via both experimental measurements[1,2] and theoretical investigations (through both atomistic calculations[3,4] and modifications to continuum theory[5–7]) indicate that the effective elastic properties of nanostructures are strongly size dependent. Due to their small size and thus the large surface-to-volume ratio, the surface stress effects have been suggested as the explanation for the size effects.[8] As a consequence, the majority of research concerning the elastic response of nanostructures have focused on surface stress[9–11] and surface elasticity[5,12,13] effects. Miller and Shenoy[5] developed a simple model to incorporate surface elasticity in an effective elastic modulus for plates and rods. Some specific examples such as plane strain, uniaxial tension, and pure bending were studied. More recently, Guo and Zhao[6,7] presented a theoretical model for elastic bending of a nanobeam with the influence of surface relaxation. The models were based on the assumption that the surface elastic properties at top and bottom surfaces are the same. Therefore, the influence of beam extension was neglected. The above assumptions become limiting for structures with a few nanometer thickness. This is because coupling stiffness arises from surface stress and surface elasticity imbalance caused by either surface reconstruction[14] or molecular adsorption[15] at top and bottom surfaces. Recently, Zang *et al.*[14] demonstrated that in an odd-layer film, there exists a surface stress imbalance between its top and bottom surface, leading to bending of the film. Molecular adsorption at one side[15] can also induce the imbalance. We add here, that there also exists a surface elasticity imbalance between its top and bottom surfaces, which is caused by reconstruction[14] or molecular adsorption[15] effects. Consequently, the often-used decoupling of bending and extensional effects is no longer valid and a bending-extensional coupling stiffness has to be accounted for.

In this letter, an extended description of surface effects induced-size dependent elastic behavior of ultrathin cantilever plates is proposed. It accounts for the bending-extensional coupling stiffness which has, so far, been ignored. The proposed model is the basis for an extension of Stoney's formula[16] for bending of cantilevers with nanoscale thickness. As an example, the elastic behavior of a Si cantilever influenced by chemisorption of H atoms[15] as a function of thickness for 1 and 2 monolayers (ML) H coverage is analyzed.

Consider a plate structure with different surface elastic properties at its top and bottom surface. Using classical plate assumptions, the tangential strain components at any point in the plate can be described as

$$\varepsilon_{\alpha\beta}(x_\rho,z)=\gamma_{\alpha\beta}(x_\rho)+z\chi_{\alpha\beta}(x_\rho),\quad \alpha,\beta,\rho=1,2, \tag{1}$$

where $\gamma_{\alpha\beta}$ are the midplane strains or membrane deformations and $\chi_{\alpha\beta}$ are the curvatures of the midplane. The transverse coordinate is z and the midplane coincides with $z=0$. In-plane coordinates are denoted as x_α, $\alpha=1,2$. The deformation of the plate can be expressed in terms of the displacements of the midplane surface via

$$\boldsymbol{\gamma}_{\alpha\beta}=\frac{1}{2}(u_{\alpha,\beta}+u_{\beta,\alpha}),\quad \boldsymbol{\chi}_{\alpha\beta}=-w_{,\alpha\beta},\quad \ldots_{,\alpha}\equiv\frac{\partial\ldots}{\partial x_\alpha}, \tag{2}$$

where u_α and w are in-plane and transverse displacement components of the midplane ($z=0$), respectively. For a compact notation it is convenient to adopt the notation

$$\boldsymbol{\gamma}=\begin{pmatrix}\gamma_{11}\\ \gamma_{22}\\ 2\gamma_{12}\end{pmatrix},\quad \boldsymbol{\chi}=\begin{pmatrix}\chi_{11}\\ \chi_{22}\\ 2\chi_{12}\end{pmatrix}. \tag{3}$$

Using linear constitutive equations, the tangential stresses follow as

a)Electronic mail: h.sadeghianmarnani@tudelft.nl.

$$\boldsymbol{\sigma} = \begin{pmatrix} \sigma_{11} \\ \sigma_{22} \\ \sigma_{12} \end{pmatrix} = \tilde{\mathbf{Q}}(\boldsymbol{\gamma} + z\boldsymbol{\chi}) + \boldsymbol{\sigma}_s. \tag{4}$$

For homogeneous and isotropic material

$$\tilde{\mathbf{Q}} = \tilde{\mathbf{Q}}^T = \frac{E}{1-\nu^2}\begin{pmatrix} 1 & \nu & 0 \\ \nu & 1 & 0 \\ 0 & 0 & \dfrac{1-\nu}{2} \end{pmatrix}. \tag{5}$$

The equivalent surface stresses are assumed to be isotropic as well, and they can be modeled as[17]

$$\boldsymbol{\sigma}_s = \boldsymbol{\sigma}^+ \delta(z - t/2) + \boldsymbol{\sigma}^- \delta(z + t/2), \tag{6}$$

where $\boldsymbol{\sigma}^+$ and $\boldsymbol{\sigma}^-$ are the surface stresses at the top and bottom surfaces of the plate, respectively, δ is the Dirac function and t is the thickness of the cantilever. The surface stresses are related to the surface deformations via

$$\boldsymbol{\sigma}^{\pm} = \boldsymbol{\sigma}_0^{\pm} + \mathbf{S}^{\pm}\left(\boldsymbol{\gamma} \pm \frac{t}{2}\boldsymbol{\chi}\right), \tag{7}$$

where $\boldsymbol{\sigma}_0^{\pm}$ are intrinsic surface stresses and $\mathbf{S}^{\pm}$ surface elasticities and can be determined from atomistic calculations.[5,13] Using Eqs. (1)–(7), tangential stress resultants and tangential stress couples, which are energetically conjugate to $\boldsymbol{\gamma}$ and $\boldsymbol{\chi}$ [see Eq. (3)], follow as

$$\mathbf{N} = \int_{-t/2}^{t/2} \boldsymbol{\sigma} dz = (\mathbf{A} + \boldsymbol{S}_\Sigma)\boldsymbol{\gamma} + \left(\mathbf{B} + \frac{t}{2}\boldsymbol{S}_\Delta\right)\boldsymbol{\chi} + \boldsymbol{\Sigma}_0^s, \tag{8}$$

$$\mathbf{M} = \int_{-t/2}^{t/2} \boldsymbol{\sigma} z dz = \left(\mathbf{B} + \frac{t}{2}\boldsymbol{S}_\Delta\right)\boldsymbol{\gamma} + \left(\mathbf{D} + \frac{t^2}{4}\boldsymbol{S}_\Sigma\right)\boldsymbol{\chi} + \frac{t}{2}\boldsymbol{\Delta}_0^s, \tag{9}$$

where

$$\boldsymbol{\Sigma}_0^s = \boldsymbol{\sigma}_0^+ + \boldsymbol{\sigma}_0^- \quad \text{and} \quad \boldsymbol{\Delta}_0^s = \boldsymbol{\sigma}_0^+ - \boldsymbol{\sigma}_0^-, \tag{10}$$

$$\boldsymbol{S}_\Sigma = \boldsymbol{S}^+ + \boldsymbol{S}^- \quad \text{and} \quad \boldsymbol{S}_\Delta = \boldsymbol{S}^+ - \boldsymbol{S}^-, \tag{11}$$

$$(\mathbf{A} \quad \mathbf{B} \quad \mathbf{D}) = \int_{-t/2}^{t/2} \tilde{\mathbf{Q}}(1 \quad z \quad z^2) dz. \tag{12}$$

Here, **A**, **B**, and **D** are extensional, bending-extensional coupling and bending stiffness, respectively. It can be easily seen that the surface stiffness leads to a modified extensional, bending-extensional coupling and bending stiffness. They can be written as

$$\mathbf{A}^* = \mathbf{A} + \boldsymbol{S}_\Sigma, \frac{E_a^* - E_a}{E_a} = \frac{\boldsymbol{S}_\Sigma}{E_a t} \quad \text{and} \quad \mathbf{B}^* = \frac{t}{2}\boldsymbol{S}_\Delta, \tag{13}$$

$$\mathbf{D}^* = \mathbf{D} + \frac{t^2}{4}\boldsymbol{S}_\Sigma, \quad \frac{E_b^* - E_b}{E_b} = \frac{3\boldsymbol{S}_\Sigma}{E_b t}, \tag{14}$$

where E_a^* and E_a are modified and classical effective Young's Modulus in extensional mode. E_b^* and E_b are modified and classical effective Young's Modulus in bending mode. It can be seen in Eqs. (13) and (14) that extensional and bending stiffness are both first-order-size-dependent but the effect of surface elasticity on bending stiffness is three times bigger than for extension. $\mathbf{B}^*$ introduce coupling between extension and bending due to surface elasticity imbalance, e.g., a nanofilm subjected to in-plane loads will tend to bend in addition to extending. For a configuration which is symmetric with respect to the midplane, the coupling terms disappear.

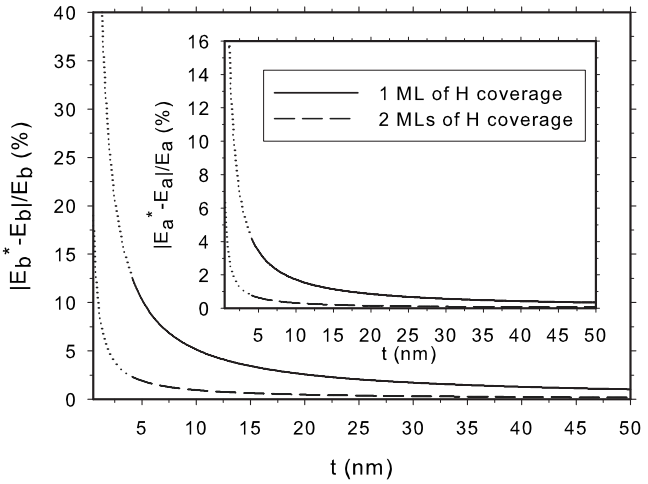

FIG. 1. Nondimensional difference between modified and classical effective Young's Modulus in bending mode as a function of thickness for 1 and 2 ML H coverage. The inset shows the difference in extensional mode.

As an example, the elastic behavior of Si cantilevers induced by chemisorption of H atoms[15] is analyzed. Zang and Liu[15] carried out the atomistic simulations for chemisorption induced surface stress imbalance and bending of Si cantilevers as a function of H coverage adsorbed on its top surface, ranging from 0 to 2 ML. When H atoms adsorb on the top surface, they induce change in surface stress and/or surface elasticity while the bottom surface still has its intrinsic values (no adsorption at the bottom surface). For 1 and 2 ML H coverages, respectively, $S^+ = S_{\mathrm{Si-H}} = 0.858$ and -0.343 eV Å^{-2} and $S^- = 0.614$ eV Å^{-2}.[15] σ_0^+ changes from -83.85 to 55.93 and -26.33 meV Å^{-2} for 0, 1, and 2 ML, respectively, and σ_0^- is -83.85 meV Å^{-2}.[15] Figure 1 shows the nondimensional difference between modified and classical effective Young's Modulus in bending mode for 1 and 2 ML H coverage. The difference in extensional mode is shown as inset in Fig. 1. However, for structures with just a few number of layers, any continuum description of surface effects may not be accurate and the atomistic simulation should be used for modeling the elastic behavior. In order to emphasize this inaccuracy, the results for thicknesses below 4 nm are shown with dotted lines. In Fig. 2, the bending-extensional coupling stiffness as a function of thickness for 1 and 2 ML H coverage has been shown. By increasing the thickness of the cantilever, a bigger coupling stiffness can be seen.

In order to determine the deflection induced by the surface stress in the absence of external loads, an extended Stoney's formula is obtained as

$$\begin{pmatrix} \boldsymbol{\gamma} \\ \boldsymbol{\chi} \end{pmatrix} = -\begin{pmatrix} \mathbf{A} + \boldsymbol{S}_\Sigma & \mathbf{B} + \dfrac{t}{2}\boldsymbol{S}_\Delta \\ \mathbf{B} + \dfrac{t}{2}\boldsymbol{S}_\Delta & \mathbf{D} + \dfrac{t^2}{4}\boldsymbol{S}_\Sigma \end{pmatrix}^{-1} \begin{pmatrix} \boldsymbol{\Sigma}_0^s \\ \dfrac{t}{2}\boldsymbol{\Delta}_0^s \end{pmatrix}. \tag{15}$$

Here, unlike the Stoney's formula, the surface stress is not constant during and after bending (the bending curvature in-

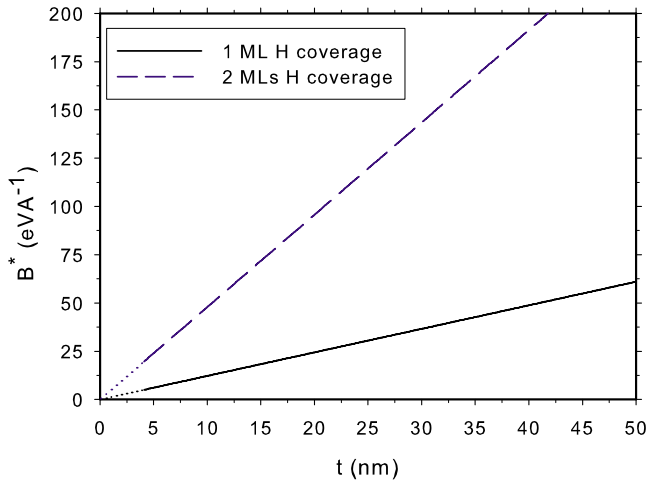

FIG. 2. (Color online) Bending-extensional coupling stiffness as a function of thickness for 1 and 2 ML H coverage. The surface elasticity imbalance induces the bending-extensional coupling.

duces the bending strain which will change the surface stress). Moreover, the curvature and the midplane strain are coupled. This implies that the often-used simplification which is the decoupling of in-plane and out-of-plane deformations is no longer applicable. Figure 3 shows the curvature provided by the extended Stoney's formula κ_m divided by that provided by classical Stoney's formula κ_S for 1 ML H coverage as a function of cantilever thickness. The inset shows the κ_m/κ_S for 2 ML H coverage.

In summary, we studied the surface stress and surface elasticity effects on the overall elastic behavior of ultrathin cantilevers. It was shown that extensional and bending stiffness components are first-order size dependent. It was shown when there is surface stress and surface elasticity imbalance, there would be an additional bending-extensional coupling stiffness. Based on this new description of extensional stiffness, bending stiffness, and bending-extensional coupling stiffness, curvature of nanocantilevers was studied which leaded to an extension of Stoney's formula. The main extension over the classical Stoney's formula is not only the effects of surface stress and surface elasticity imbalance, but also the effect of in-plane deformations on out-of-plane deformations. It should be added here that since the surface region is only a few atomic layers thick atomistic simulations are inevitably involved to include the surface effects in modeling the nanostructures. On the other hand, the large difference in length scale is a fundamental issue that should be included in any modeling of macroscopic behavior of nanostructures.

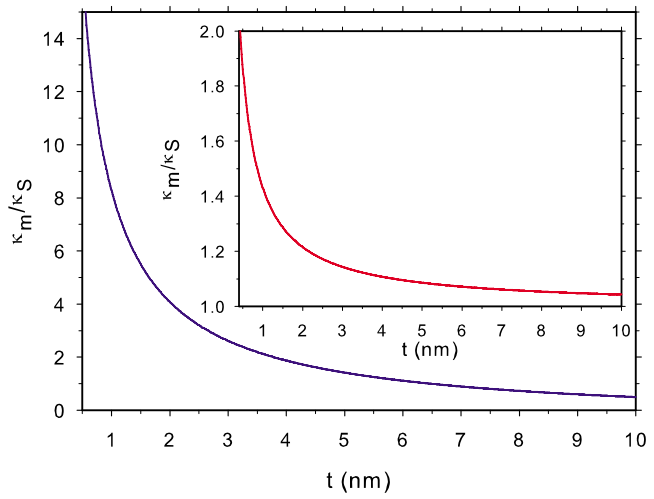

FIG. 3. (Color online) The κ_m/κ_S caused by 1 ML H coverage as a function of thickness. The inset shows the ratio for 2 ML H coverage.

The framework proposed in this letter can be seen as the link between the atomistic nature of the surface effects and the elastic behavior. On the other hand, one should bear in mind that at what characteristic length scale the continuum elasticity ceases to accurately describe the mechanical behavior. It is clear that below that length scale, the continuum description of surface effects may not be accurate. The studied example involved Si nanocantilevers, but can be generalized to other semiconductor nanofilms.

This work was done as part of Dutch national research program on micro technology, MicroNed project code: IV-C-2.

[1]S. Cuenot, C. Frétigny, S. Demoustier-Champagne, and B. Nysten, Phys. Rev. B **69**, 165410 (2004).
[2]R. Agrawal, B. Peng, E. Gdoutos, and H. D. Espinosa, Nano Lett. **8**, 3668 (2008).
[3]G. Cao and X. Chen, Phys. Rev. B **76**, 165407 (2007).
[4]L. G. Zhou and H. Huang, Appl. Phys. Lett. **84**, 1940 (2004).
[5]R. E. Miller and V. B. Shenoy, Nanotechnology **11**, 139 (2000).
[6]J.-G. Guo and Y.-P. Zhao, J. Appl. Phys. **98**, 074306 (2005).
[7]J.-G. Guo and Y.-P. Zhao, Nanotechnology **18**, 295701 (2007).
[8]M. Schmid, W. Hofer, P. Varga, P. Stoltze, K. W. Jacobsen, and J. K. No/rskov, Phys. Rev. B **51**, 10937 (1995).
[9]M. J. Lachut and J. E. Sader, Phys. Rev. Lett. **99**, 206102 (2007).
[10]K. S. Hwang, K. Eom, J. H. Lee, D. W. Chun, B. H. Cha, D. S. Yoon, T. S. Kim, and J. H. Park, Appl. Phys. Lett. **89**, 173905 (2006).
[11]J. Dorignac, A. Kalinowski, S. Erramilli, and P. Mohanty, Phys. Rev. Lett. **96**, 186105 (2006).
[12]G.-F. Wang and X.-Q. Feng, Appl. Phys. Lett. **90**, 231904 (2007).
[13]P. Lu, H. P. Lee, C. Lu, and S. J. O'Shea, Phys. Rev. B **72**, 085405 (2005).
[14]J. Zang, M. Huang, and F. Liu, Phys. Rev. Lett. **98**, 146102 (2007).
[15]J. Zang and F. Liu, Nanotechnology **18**, 405501 (2007).
[16]G. G. Stoney, Proc. R. Soc. London, Ser. A **82**, 172 (1909).
[17]J. E. Sader, J. Appl. Phys. **89**, 2911 (2001).